



DOI: 10.18720/MCE.94.6

## Intake rate through openings in the side wall of the duct

**D.V. Maklakov<sup>a</sup>, V.N. Posohin<sup>b</sup>, R.G. Safiullin<sup>b</sup>, J.R. Kareeva<sup>\*b</sup>**

<sup>a</sup> Kazan (Volga region) Federal University, Kazan, Russia

<sup>b</sup> Kazan State University of Architecture and Engineering, Kazan, Russia

\* E-mail: [jkareeva2503@gmail.com](mailto:jkareeva2503@gmail.com)

**Keywords:** intake ducts, openings in the side wall, intake rate, ideal fluid, conformal mappings, numerical calculation

**Abstract.** Subject. In technological and general ventilation ducts with a given uniformity of intake is often needed to be designed. The calculation of pressure losses in such ducts is complicated by the lack of reliable information about the characteristics of the flows at the inlet to the intake openings and slots. Intensity of air intake through slot openings located on one and two opposite walls of the duct in a series of sequentially placed slots, which determines the presence of a transit air stream passing by the hole is calculated. The slots are perpendicular to the generatrix panel and can be opposite or offset relative to each other. The presence of a stagnant zone formed when the flow is cut off from a sharp edge at the inlet is taken into account. Methods. The search for a solution is carried out in the framework of ideal fluid jets theory using the Kirchhoff scheme and Chaplygin method of singularities, as well as by the numerical method using Flow3d software package, where the system of equations of plane turbulent motion was ended with “standard” k-e model. Results. The flow rates of the air entering through the slots were found, depending on their width and value of the transit flow. Dependencies for the attached flow with and without flow separation are obtained. The shape of the free streamline separating the jet and vortex zones, the compression coefficients of the jet are determined. Current flow lines are constructed for different values of the geometric parameters of the duct and the hole. Conclusion. Analytical and numerical calculations showed that the kinematics of currents and values of the attached flow rate are very similar, but the size and shape of the stagnant zone are significantly different. A numerical solution gives more physics of stagnant zone formation. It was found that flow separation reduces the associated flow rate. It was also found that the intensity of absorption is minimal with the opposite order of cracks.

### 1. Introduction

The intake of air through slots or a series of local openings of various shapes (round, square, slotted) in the side wall when exposed to intense transit flow is a typical task for many technical devices. For example, it is used when calculating cooling of the turbine blades surface [1], during the operation of ejectors [2, 3]. In technological applications of ventilation, there is often a need to design ducts with a given uniformity (nonuniformity) of intake along the length. Failure to comply with the specified intake conditions can lead to ineffective local intake from sources of harmful emissions, a violation of regulations for the operation of technological equipment, etc. [3–10]. Uniform intake ducts (USD) are also used in public buildings to remove air from the upper zone by general ventilation.

Depending on the current task, uniform intake along the entire length can be achieved by selecting the optimal hole sizes and distances between them. With sufficient length, such air ducts are more technologically advanced and economical in comparison with air ducts having variable parameters. The main characteristic of the energy-efficient choice of geometry and location of the openings in the USD is the local resistance coefficient (LRC) of its main perturbing elements. The analytical determination of USD flow parameters, which are important for calculating the LRC (associated flow rate, intake rate, stream compression ratio, flow stream lines, shape and size of stagnant zones), is very difficult, because when entering through openings and slots, air loses energy in the opening itself, and when passing through the duct near such a hole. Therefore, the LRC values are determined, as a rule, experimentally. A large amount of LRC data is contained in the well-known Reference book on hydraulic resistance by I.E. Idelchik [11], which has already been published in four editions in 1960, 1975, 1992 and 2005. But this fundamental work is far from exhausting the whole variety of

Maklakov, D.V., Posohin, V.N., Safiullin, R.G., Kareeva, J.R. Intake rate through openings in the side wall of the duct. Magazine of Civil Engineering. 2020. 94(2). Pp. 65–80. DOI: 10.18720/MCE.94.6



This work is licensed under a [CC BY-NC 4.0](https://creativecommons.org/licenses/by-nc/4.0/)

constructive situations encountered in practice. In these handbooks there is no data on separation zones, compression ratios of flow at the entrance and passage through the side openings of the air-blast.

Significant simplifications introduced in the USD analysis in the well-known works on this topic [13] do not make it possible to consider this problem as a solved one, and theoretical and experimental studies of transit ducts with constant parameters of channel and slot or channel and side openings are relevant. Therefore, now there still appear works devoted to the study of USD currents, for example. In these works, the authors use numerical experiment using computational fluid dynamics methods. Modern software systems, such as Fluent [13], Flow3d [14], which implement computational fluid dynamics methods, allow one to study such flows quite accurately and in detail. However, the accuracy and adequacy of results obtained by such methods should be monitored by comparison with already known and reliable methods.

The paper considers methods for calculating flows during intake through a series of slit-like openings, which can be located on one or two opposite walls of the duct. The purpose of the calculation is to determine the intensity of absorption through the holes for different geometric situations, as well as the flow parameters necessary to calculate the CLR of the flow in the turbine fouling (connected flow rate, absorption rate, stream compression ratio, flow stream lines, shape and size of stagnant zones). The analysis is carried out within the framework of the ideal fluid flow model and numerically taking into account viscosity  $C$  using Flow3d software package.

## 2. Methods

### 2.1. Hole on one side of the intake duct wall

A flow diagram is given in Figure 1a where  $l$  – long CA slot in the wall of the intake duct with height  $h$  (Figure 1a). Transit airflow from overlying openings moves with velocity  $v_\infty$ , accordingly, specific transit flow is  $q_0 = v_\infty h$ . It is necessary to determine the intensity of air intake  $\Delta q_0$  through the gap (adjoined flow rate) and construct the currents flow lines.

#### 2.1.1. Ideal fluid, unseparated flow

First, we consider the unseparated flow model (Figure 1, a), which does not take into account the fact of formation of a weakly-vortex (stagnant) zone when stream flows around a sharp edge A. We will find the solution using the conformal mapping method [15, 16].

As a parametric region, we take the upper half-plane  $t = \xi + i\eta$  with the location of points indicated in Figure 1, a, b. The flow region in the plane of complex potential  $w = \phi + i\psi$  is shown in Figure 1, c.

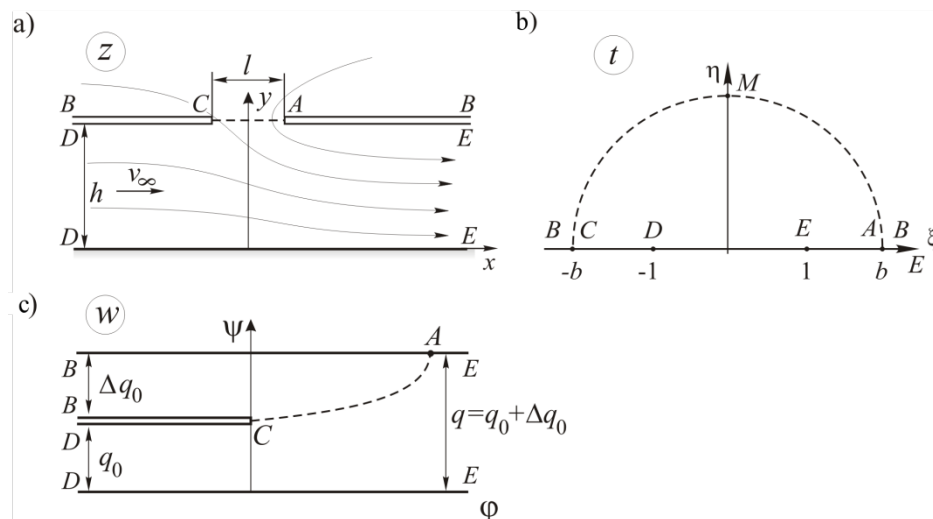


**Figure 1. Flow areas for unseparated flow model: a is physical plane  $z = x + iy$ ; b is parametric plane  $t = \xi + i\eta$ ; c is plane of complex potential  $w = \phi + i\psi$**

The matching between the flow areas in the  $z$  and  $t$  planes is established using the Christoffel-Schwartz formula [15]

$$\frac{dz}{dt} = c \frac{t^2 - b^2}{t^2 - 1},$$

where  $c$  and  $b$  are the mapping parameters.

After integration the following expression is obtained:

$$z = c \left[ t + \frac{1-b^2}{2} \ln \frac{t-1}{t+1} - \frac{1-b^2}{2} \pi i \right]. \quad (1)$$

At the point  $D$  ( $t = -1$ ), the function  $dz/dt$  has a first order pole. By determining the residue of function at this point, we obtain

$$h = c\pi \frac{b^2 - 1}{2}, \quad (2)$$

and find the final form of the mapping formula

$$z = \frac{h}{\pi} \left[ \frac{2t}{b^2 - 1} + \ln \frac{t+1}{t-1} \right] + iH. \quad (3)$$

At points  $A$  and  $C$  we have

$$z_A = z(b) = c \left( b + \frac{1-b^2}{2} \ln \frac{b-1}{b+1} - \frac{1-b^2}{2} \pi i \right);$$

$$z_C = z(-b) = c \left( -b + \frac{1-b^2}{2} \ln \frac{b+1}{b-1} - \frac{1-b^2}{2} \pi i \right).$$

Consequently,

$$z_A - z_C = l = 2c \left( b + \frac{b^2 - 1}{2} \ln \frac{b+1}{b-1} \right)$$

and further

$$c = \frac{l}{2} \left( b + \frac{b^2 - 1}{2} \ln \frac{b+1}{b-1} \right)^{-1}. \quad (4)$$

From equations (2), (4) we obtain the formula for determining the parameter  $b > 1$

$$\frac{l}{h} = \frac{2}{\pi} \left( \frac{2b}{b^2 - 1} + \ln \frac{b+1}{b-1} \right). \quad (5)$$

Further we find the equation of the  $AC$  line in the parametric plane  $t = \xi + i\eta$ . It is a consequence of the expression

$$\operatorname{Im} \left[ \frac{2t}{b^2 - 1} + \ln \frac{t+1}{t-1} \right] = 0.$$

Having completed the necessary transformations, we obtain

$$\xi = \pm \sqrt{2\eta \operatorname{ctg} \frac{2\eta}{b^2 - 1} + 1 - \eta^2}, \quad 0 \leq \eta < \eta_M, \quad (6)$$

where  $\eta_M > 0$  is determined from the equation  $2\eta_M \operatorname{ctg} \frac{2\eta_M}{b^2 - 1} + 1 - \eta_M^2 = 0$ .

Note that for large values of  $b$ , from formula (6) it follows that the line  $BE$  in the parametric plane is determined by equation (at  $b \rightarrow \infty$ )  $\xi = \pm \sqrt{b^2 - \eta^2}$ , that is, this line is almost a circle of radius  $b$ .

On the segment  $AC$

$$\bar{y} = \frac{y}{h} = 1, \quad \bar{x} = \frac{x}{h} = \pm \frac{1}{\pi} \left[ \frac{2\xi}{b^2 - 1} + \ln \frac{\sqrt{(\xi^2 + \eta^2 - 1)^2 + 4\eta^2}}{(\xi - 1)^2 + \eta^2} \right], \quad |\xi| > b, \quad 0 \leq \eta < \eta_M. \quad (7)$$

In the plane  $t$ , we have sources at points  $D$  ( $t = -1$ );  $B$  ( $t = \infty$ ) and drain at  $E$  ( $t = 1$ ). The complex potential of such a flow will be

$$w = \frac{q_0}{\pi} \ln(t+1) - \frac{q_0 + \Delta q_0}{\pi} \ln(t-1) = \frac{q_0}{\pi} \left[ \ln(t+1) - (1 + C_q) \ln(t-1) \right], \quad (8)$$

where  $C_q = \Delta q_0 / q_0$  is the dimensionless adjoined flow.

The complex adjoined velocity is

$$v_x - iv_y = \frac{dw}{dt} \cdot \frac{dt}{dz} = \frac{q_0}{\pi} \cdot \frac{(t-1) - (1+C_q)(t+1)}{t^2 - b^2}. \quad (9)$$

By defining residues of function  $dw/dt$  at points  $D$  and  $B$ , we find the dimensionless adjoined flow

$$C_q = \frac{2}{b-1}. \quad (10)$$

By separating the real and imaginary parts of equalities (8), (9), we find the equations for the flow function

$$\psi = \frac{q_0}{\pi} \left[ \operatorname{arcCos} \frac{\xi+1}{\sqrt{(\xi+1)^2 + \eta^2}} - (1+C_q) \operatorname{arcCos} \frac{\xi-1}{\sqrt{(\xi-1)^2 + \eta^2}} \right], \quad (11)$$

and for the flow velocity components:

$$v_x = \frac{q_0}{\pi c} \cdot \frac{[\xi-1 - (1+C_q)(\xi+1)] \cdot (\xi^2 - \eta^2 - b^2) + 2\xi\eta^2 C_q}{(\xi^2 - \eta^2 - b^2)^2 + 4\xi^2\eta^2}, \quad (12)$$

$$v_y = \frac{q_0}{\pi c} \cdot \frac{2\xi\eta [1 - \xi + (1+C_q)(1+\xi)] - C_q\eta(\xi^2 - \eta^2 - b^2)}{(\xi^2 - \eta^2 - b^2)^2 + 4\xi^2\eta^2}, \quad (13)$$

where  $\xi \geq 0$ ,  $\eta \geq 0$ .

We let us consider the problem of an ideal fluid flow, taking into account the separated flow (the diagram is shown in Figure 2 a). At point  $A$ , the flow breaks away from the wall, forming a stagnant (weakly vortex) zone. The velocity at the free  $AE$  boundary is  $v_0$ . At point  $C$ , the leakage rate is finite. As before, it is necessary to determine the adjoined flow rate and construct the flow stream lines. We will find the general solution to the problem by the method of singular points of S.A. Chaplygin [15]. As a parametric region, we choose the upper right quadrant with the corresponding points shown in Figures 2, a, b.

We construct the function  $dw/dt$ , which is a the complex conjugate velocity of the imaginary flow in the parametric plane. We take into account that the fluid flows from the infinitely distant points  $B$ ,  $D$  and is absorbed at the infinitely distant point  $E$ , that is, the streamlines start at points  $B$ ,  $D$  and close at point  $E$ . There exist a separation point  $C$ , where the general streamline is perpendicular to the axis  $\xi$ .

We define the features of the function  $dw/dt$ . At points  $A$  and  $C$ , the right angles are flowed around, so  $t_A = 0$ ,  $t_c = c$  are zeros of the first order. Points  $E$  lie at infinity; therefore, they do not participate in the construction of the function  $dw/dt$ . At points  $B$  ( $t_B = b$ ) and  $D$  ( $t_D = 1$ ) we have the poles of the first order.

We analytically continue  $dw/dt$  on the entire complex plane. On the real axis  $\xi$  the condition  $\operatorname{Im} \frac{dw}{dt} = 0$  is satisfied. According to the principle of symmetry, we analytically continue  $dw/dt$  through this axis to the lower right quadrant, with no additional features. On the imaginary axis  $\eta$  the condition  $\operatorname{Re} \frac{dw}{dt} = 0$  is satisfied that allows one to analytically continue  $dw/dt$  on the whole complex plane. Moreover, at the point  $C$  ( $t_c = -c$ ) we get zero, and at the points  $B$  ( $t_B = -b$ ) and  $D$  ( $t_D = -1$ ) we obtain the first order poles.

As a result of these continuations, the function  $dw/dt$  is built in the form

$$\frac{dw}{dt} = \phi_0 \frac{t(t^2 - c^2)}{(t^2 - 1)(t^2 - b^2)} = \phi_0 f(t). \tag{14}$$

On ADE  $\text{Im} \frac{dw}{dt} = 0$  and therefore, is a real number.

The picture of the flow lines of an imaginary flow in the parametric plane, constructed using the *StreamPlot* option of the *Mathematica* software [14], is shown in Figure 3.

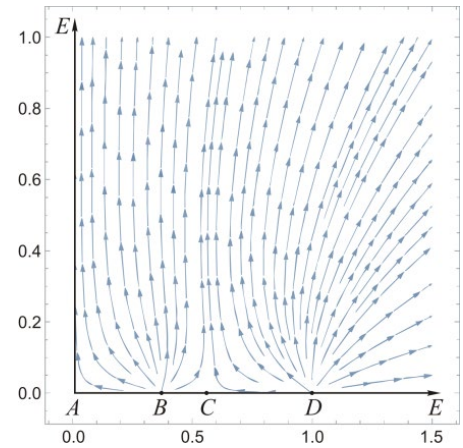
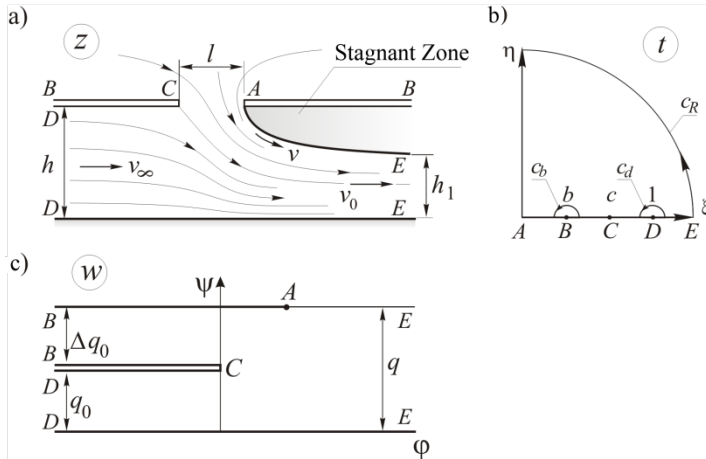


**Figure 2. Flow areas for separated flow model:**  
**a is physical plane  $z = x + iy$ ; b is parametric plane  $t = \xi + i\eta$ ; c is plane of complex potential  $w = \phi + i\psi$ .**

**Figure 3. Imaginary flow.**

We construct a function  $\frac{dw}{dz} = \frac{v_x}{v_0} - i \frac{v_y}{v_0}$ . This function has a unique zero at the point  $t = b$ , which, after

analytic continuation through the imaginary axis, turns into a pole at the point  $t = -b$ , since  $\left| \frac{dw}{v_0 dz} \right| = 1$  on the

imaginary axis. Given that with  $t \rightarrow \infty \frac{dw}{v_0 dz} = 1$ , we obtain

$$\frac{dw}{v_0 dz} = \frac{t - b}{t + b}.$$

Next, we find the derivative of the mapping function  $z = z(t)$

$$q = v_0 h_1 \frac{dz}{dt} = \frac{dz}{dw} \cdot \frac{dw}{dt} = \frac{\phi_0}{v_0} \frac{t(t^2 - c^2)}{(t^2 - 1)(t^2 - b^2)} \cdot \frac{t - b}{t + b} = \frac{\phi_0}{v_0} F(t). \tag{15}$$

The expressions (14), (15), in principle, allow constructing streamlines in the parametric and physical planes.

We proceed to determine the flow rate of air sucked through the gap. The flow rate at point  $D$  is  $q_0 = v_\infty h$ , and at point  $E$  it is  $q = v_0 h_1$ , so flow through the gap is  $\Delta q_0 = q - q_0$ .

Function  $dw/dt$  is analytical in the upper right quadrant, excluding points  $B, C, E$ . Points  $B, C$  on the parametric plane are marked by semicircles of infinitely small radius; we surround the remote point  $E$  with a quarter of a circle of infinitely large radius (Figure 2, b). When switching from  $DC$  to  $DE$  in a semicircle  $C_d$   $\text{Im } w$  experiences a jump  $q_0$  (Figure 2, c).

Using the residue theorem, we find

$$iq_0 = \oint_{C_d} \frac{dw}{dz} dz = \pi i \text{res}_{t=1} [\phi_0 f(t)] = \pi i \phi_0 \frac{1 - c^2}{2(1 - b^2)},$$

whence it follows that the transit flow intensity is

$$q_0 = \pi\phi_0 \frac{1-c^2}{2(1-b^2)}. \quad (16)$$

When moving from  $BC$  to  $BA$  in a semicircle  $C_b$   $Im w$  experiences a jump  $\Delta q_0$ , hence

$$i\Delta q_0 = \oint_{C_b} \frac{dw}{dt} dt = \pi i \operatorname{res}_{t=b} [\phi_0 f(t)] = \pi i \phi_0 \frac{b^2 - c^2}{2(b^2 - 1)},$$

and the intensity of flow entering the gap is

$$\Delta q_0 = \pi\phi_0 \frac{b^2 - c^2}{2(b^2 - 1)}, \quad (17)$$

when switching from  $DE$  to  $AE$  in a quarter circle  $C_R$   $Im w$  experiencing a jump  $q$  and

$$iq = \oint_{C_R} \frac{dw}{dt} dt = \frac{\pi}{2} i \operatorname{res}_{t=\infty} [\phi_0 f(t)] = \phi_0 i \frac{\pi}{2},$$

which means the intensity of the total flow

$$q = \frac{\pi\phi_0}{2}. \quad (18)$$

From formulas (16)-(18) we find the dimensionless associated flow

$$C_q = \frac{\Delta q_0}{q_0} = \frac{q}{q_0} - 1 = \frac{1-b^2}{1-c^2} - 1. \quad (19)$$

Now we determine the sizes  $h$  and  $h_1$ . When switching from  $DC$  to  $DE$  by semicircles  $c_d$   $Im z$  experiences a jump  $h$ . From here

$$ih = \oint_{c_d} \frac{dz}{dt} dt = \frac{\phi_0}{v_0} \pi i \operatorname{res}_{t=1} F(t) = \frac{\phi_0}{v_0} \pi i \frac{1-c^2}{2(1-b^2)},$$

$$h = \frac{\phi_0}{v_0} \pi \frac{1-c^2}{2(1-b^2)}, \quad (20)$$

when switching from  $DE$  to  $AE$  in a quarter circle  $c_R$   $Im z$  experiences a jump  $h_1$  and it means that

$$ih_1 = \oint_{c_R} \frac{dz}{dt} dt = \frac{\phi_0}{v_0} \frac{\pi i}{2} \operatorname{res}_{t=\infty} F(t) = \frac{\phi_0}{v_0} \frac{\pi i}{2},$$

$$h_1 = \frac{\phi_0}{v_0} \frac{\pi}{2}. \quad (21)$$

Combining expressions (20), (21) we find the compression ratio of the flow

$$K = \frac{h_1}{h} = \frac{(1-b)^2}{1-c^2}. \quad (22)$$

It remains to determine the mapping parameters  $b$ ,  $c$  and the coefficient  $\phi_0$ . Since point  $B$  in the physical plane at infinity to the left and to the right of the gap is at the same level, then

$$\operatorname{Im} \oint_{t=b} \frac{dz}{dt} dt = 0 \Rightarrow \operatorname{res}_{t=b} F(t) = 0. \quad (23)$$

On the other hand

$$\operatorname{res}_{t=b} F(t) = \frac{d}{dt} \left[ \frac{t(t^2 - c^2)}{t^2 - 1} \right]_{t=b} = 0.$$

We take the logarithmic derivative

$$\frac{d}{dt} \ln \frac{t(t^2 - c^2)}{t^2 - 1} \Big|_{t=b} = \left[ \frac{1}{t} + \frac{2t}{t^2 - c^2} - \frac{2t}{t^2 - 1} \right]_{t=b} = 0$$

From the previous equalities it follows

$$\frac{1}{b} + \frac{2b}{b^2 - c^2} - \frac{2b}{b^2 - 1} = 0$$

and

$$c = b \sqrt{\frac{3 - b^2}{1 + b^2}}. \quad (24)$$

From the graph of function (24) (Figure 4) it can be seen that for  $0 < b < 1$ , the following is always true:  $b < c < 1$ .

The function  $F(t) = \frac{t(t^2 - c^2)}{(t^2 - 1)(t^2 - b^2)}$ , entering the mapping formula (15), will be decomposed to a sum of partial fractions

$$F(t) = \frac{M}{t-1} + \frac{N}{t+1} + \frac{P}{(t-b)^2} + \frac{K}{t-b}.$$

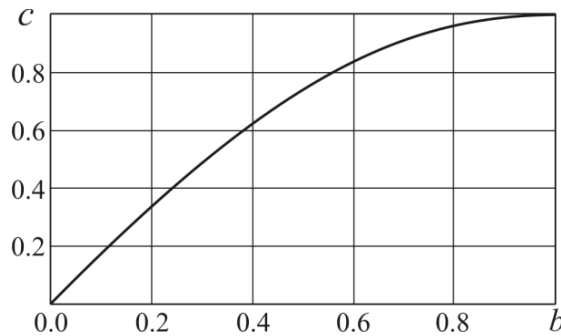


Figure 4. Plot of function  $c = c(b)$ .

In view of (23) the coefficient  $K = 0$ , for other coefficients we get

$$\left. \begin{aligned} M &= \oint_{t=1} \frac{dz}{dt} dt = \operatorname{res}_{t=1} F(t) = \frac{1 - c^2}{2(1 - b)^2} \\ B &= \oint_{t=-1} \frac{dz}{dt} dt = \operatorname{res}_{t=-1} F(t) = \frac{1 - c^2}{2(1 + b)^2} \\ C &= \oint_{t=b} \frac{dz}{dt} dt = \frac{b(b^2 - c^2)}{b^2 - 1} \end{aligned} \right\} \quad (25)$$

We find the primitive for function  $F(t)$

$$G(t) = \int F(t) dt = M \ln(t-1) + N \ln(t+1) - \frac{P}{t-b}. \quad (26)$$

For the parametric plane the slot of the width  $l$  corresponds to a segment  $AC$

$$l = \frac{\phi_0}{v_0} \operatorname{Re} [G(0) - G(c)].$$

Using the expression (20), we obtain

$$\frac{l}{h} = \frac{2(1-b)^2}{\pi(1-c^2)} \operatorname{Re} [G(0) - G(c)]. \quad (27)$$

So, to find  $b$  and  $c$ , which meet the criteria  $0 < b < c < 1$ , one should solve a system of equations (24)–(27). By combining them, we get

$$\frac{(1-b)^2}{(1+b)^2} \cdot \frac{4b^2c + (b-c) \left[ (1+b^2) \ln(1-c) + (1-b^2) \ln(1+c) \right]}{\pi(c-b)(1-c^2)} = \frac{l}{h}. \quad (28)$$

The equation (28) is solved using the *Find\_Root* of the *Mathematica* software, and the parameter  $c$  is defined using the formula (24).

Let  $v_0 = 1$ ,  $h = 1$ . We introduce notations:

$$M_1 = M\phi_0, \quad N_1 = N\phi_0, \quad -P_1 = P\phi_0.$$

Taking into account (20), (25), (28) we obtain

$$M_1 = \frac{1}{\pi}, \quad N_1 = \frac{(b-1)^2}{\pi(b+1)^2}, \quad P_1 = \frac{4b^2}{\pi(b+1)^2}.$$

As point  $A$  has coordinates  $(1/2, 0)$ , we have a conformal mapping of the parametric plane onto the physical plane in the form

$$z(t) = \frac{1}{\pi} \ln(t-1) + \frac{(b-1)^2}{\pi(b+1)^2} \ln(t+1) - \frac{4b^2}{\pi(b+1)^2} - i + \frac{1}{2}. \quad (29)$$

We proceed to the construction of streamlines. This is easier to perform in the parametric plane, and then, using the conformal mapping (29), to transfer them to the physical plane. The imaginary flow in the parametric plane has velocities

$$v_\xi = v_\xi(\xi, \eta) = \phi_0 \operatorname{Re} [f(\xi + i\eta)],$$

$$v_\eta = v_\eta(\xi, \eta) = -\phi_0 \operatorname{Im} [f(\xi + i\eta)].$$

Since the imaginary flow is steady, the streamlines coincide with the particle trajectories. Therefore, the differential equations of streamlines will be

$$\xi'(\tau) = v_\xi[\xi(\tau), \eta(\tau)], \quad \eta'(\tau) = v_\eta[\xi(\tau), \eta(\tau)], \quad (30)$$

where  $\tau$  is the time of particles motion in the parametric plane.

We construct  $N$  streamlines of the transit flow. Initial conditions must be added to the system of differential equations (30). On the semicircle  $C_d$  of a small radius  $\varepsilon_1$ , we arrange  $N$  points. The initial conditions are formulated as

$$\xi(0) = \varepsilon_1 \cos \frac{\pi j}{N+1} + 1, \quad \eta(0) = \varepsilon_1 \sin \frac{\pi j}{N+1}, \quad j = \overline{1 \dots N}, \quad (31)$$

Using *NDSolve* program of the *Mathematica* software the Cauchy problem (30), (31) was solved on the interval  $\tau \in [0, \tau_{\max}]$ . As a result, we obtain the coordinates of streamlines in the parametric plane



$$\xi = \xi(\tau), \quad \eta = \eta(\tau), \quad \tau \in [0, \tau_{\max}].$$

The values  $\tau_{\max}$  were determined from a numerical experiment.

The problem described above for a viscous fluid was solved numerically by Flow3d software package. The system of equations for plane turbulent motion of a viscous fluid was closed using the "standard"  $k$ - $\varepsilon$  model ( $k$  is the kinetic energy of turbulence,  $\varepsilon$  is the dissipation rate  $k$ ). For flow zones in the immediate vicinity of the duct walls, standard wall functions were used.

At the boundaries of the computational domain, the following boundary conditions were adopted (see Figure 1, a):

- On DD, the condition for uniform distribution and constancy of velocity  $\vec{v}_{\infty}$  in the positive direction of the  $x$  axis corresponding to a given specific intensity  $q_0$ ;
- On EE, the condition for a smooth continuation of the flow through the boundary (normal derivatives at the boundary for all quantities are equal to zero);
- At the permeable boundaries of the area of air leakage to the gap, the excessive static pressure  $\Delta P = 0$ ;
- On the boundaries  $BC, AB, DE$ , solid impermeable walls on which the condition of adhesion (non-slip) is fulfilled  $\vec{v}_{\tau} = 0$ .

The temperature at all boundaries is equal to air temperature of 293K.

The total number of grid cells in the channel is 80 thousand, along the length of the slotted hole it is at least 20, as it is recommended in [14]. The channel length to the slot hole was taken equal to  $3h$  in order to exclude the influence of boundary conditions in the  $DD$  section on the flow near the slot hole. The length of the channel after the slot hole was taken to be at least  $10h$  to smooth the flow deformation due to adjoining of the flow through the slot and separation of flow from the sharp edge, which affects the accuracy of determining the total flow rate  $q = q_0 + \Delta q_0$ .

## 2.2. Bilateral arrangement of slotted openings in the duct

An element of the intake panel with a two-sided arrangement of slotted openings is shown in Figure 5 a. Transit flow from upstream openings has velocity  $v_{\infty}$ . Here it is also necessary to determine the flow rates of air entering through the slots and to build the flow stream lines.

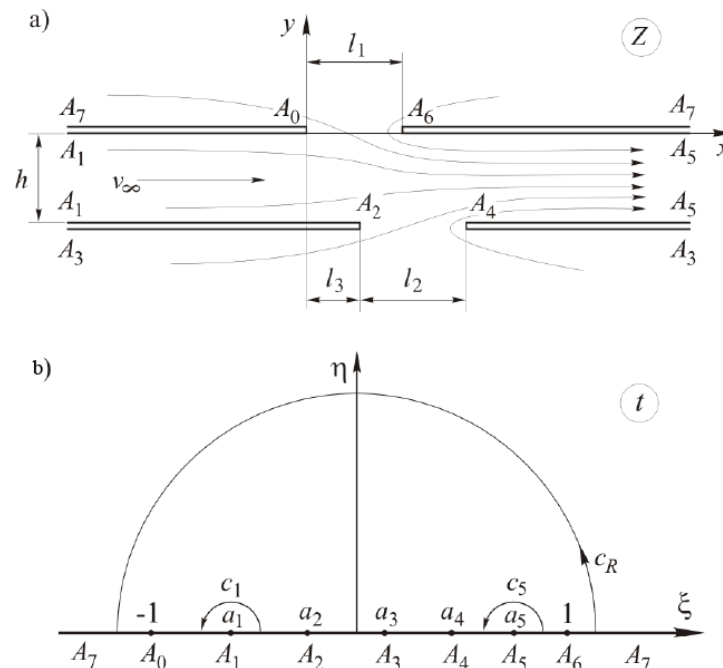


**Figure 5. Flow areas: a) physical plane  $z = x + iy$ ; b) parametric plane  $t = \xi + i\eta$ .**

Ideal fluid, unseparated flow. We find the solution using the theory of potential flows of ideal fluid by the method of conformal mappings. We do not take into account the presence of vortex zones in the places of

boundaries fractures (points  $A_4, A_6$ ). We assume that at points  $A_0$  and  $A_2$  the Kutta-Joukowski condition of the limited velocity [20] is satisfied.

We will construct the flow in the parametric region, which in our case will be the upper half-plane with the correspondence of points shown in Figure 7a, b. The relationship between the flow regions in the  $z$  and  $t$  planes is established using the Christoffel – Schwartz formula

$$z = A \int_{-1}^t F(u) du; \quad F(t) = \frac{(t^2 - 1)(t - a_2)(t - a_4)}{(t - a_1)(t - a_3)^2(t - a_5)}, \quad (32)$$

where  $u$  is the integration variable.

The mapping parameters  $a_1, a_2, a_3, a_4, a_5$  and coefficient  $A$  must be defined. We expand the function  $F(t)$  at the sum of simple rational fractions

$$F(t) = \frac{\alpha}{t - a_1} + \frac{\alpha_1}{t - a_5} + \frac{\beta}{(t - a_3)^2} + \frac{\beta_1}{t - a_3} + 1,$$

where coefficients  $\alpha, \alpha_1, \beta, \beta_1$  are real. The coefficient  $A$  is also real and positive, since for  $A_6A_7$  we have  $dx/d\xi > 0$ .

In order to obtain the same duct width at points  $A_1$  and  $A_5$ , the following conditions must be met

$$\operatorname{Im} \int_{C_1} \frac{dz}{dt} = ih \quad \text{and} \quad \operatorname{Im} \int_{C_5} \frac{dz}{dt} = -ih,$$

where  $C_1$  and  $C_5$  are semicircles of infinitely small radius, surrounding points  $A_1$  and  $A_5$  in the parametric plane  $t$  (see Figure 7, b).

Using the residue theorem, we obtain

$$\begin{aligned} \operatorname{Im} \int_{C_1} \frac{A\alpha dt}{t - a_1} = ih &\rightarrow A\alpha\pi i = ih \rightarrow A\alpha = \frac{h}{\pi}; \\ \operatorname{Im} \int_{C_5} \frac{A\alpha_1 dt}{t - a_5} = -ih &\rightarrow A\alpha_1\pi i = -ih \rightarrow A\alpha_1 = -\frac{h}{\pi}. \end{aligned}$$

It follows that

$$A = \frac{h}{\alpha\pi} = -\frac{h}{\alpha_1\pi}; \quad (33)$$

$$\alpha_1 + \alpha = 0. \quad (34)$$

In order to have the straight lines  $A_7A_0, A_6A_7$  at the same level in the physical plane, we additionally use the condition

$$\operatorname{Im} \int_{C_R} \frac{dz}{dt} = 0 \rightarrow \operatorname{Im} \int_{C_R} F(t) dt = 0, \quad (35)$$

or otherwise

$$\operatorname{Im} \left[ \int_{C_R} \frac{\alpha dt}{t - a_1} + \int_{C_R} \frac{\alpha_1 dt}{t - a_5} + \int_{C_R} \frac{\beta_1 dt}{t - a_3} + \int_{C_R} \frac{\beta dt}{(t - a_3)^2} + \int_{C_R} dt \right] = 0,$$

where  $C_R$  is the semicircle of an infinitely large radius surrounding the point  $A_7$  in the parametric plane (see Figure 5, b).

According to the residue theorem  $\int_{C_R} \frac{\beta dt}{(t - a_3)^2} = 0$ , and besides,  $\operatorname{Im} \int_{C_R} dt = 0$ , which means  $\pi i\alpha + \pi i\alpha_1 + \pi i\beta_1 = 0$ . Taking into account expression (34),  $\beta_1 = 0$ , and the function  $F(t)$  takes the form

$$F(t) = \frac{\alpha}{t-a_1} - \frac{\alpha}{t-a_5} + \frac{\beta}{(t-a_3)^2} + 1.$$

Having determined the residues of function  $F(t)$  at points  $A_1, A_5$  and the limit of function value  $F(t)(t-a_3)^2$  at  $t \rightarrow a_3$ , we express the coefficients  $\alpha, \alpha_1, \beta$  through mapping parameters  $a_1, a_2, a_3, a_4, a_5$

$$\alpha = \frac{(a_1^2 - 1)(a_1 - a_2)(a_1 - a_4)}{(a_1 - a_3)^2(a_1 - a_5)}; \quad \alpha_1 = \frac{(a_5^2 - 1)(a_5 - a_2)(a_5 - a_4)}{(a_5 - a_3)^2(a_5 - a_1)};$$

$$\beta = \frac{(a_3^2 - 1)(a_3 - a_2)(a_3 - a_4)}{(a_3 - a_1)(a_3 - a_5)}.$$

Using condition (3) from the first two expressions we find

$$\frac{(a_1^2 - 1)(a_1 - a_2)(a_1 - a_4)}{(a_1 - a_3)^2} - \frac{(a_5^2 - 1)(a_5 - a_2)(a_5 - a_4)}{(a_5 - a_3)^2} = 0. \quad (36)$$

Now consider the condition  $\text{Im} \int_{C_R} F(t) dt = 0 \rightarrow \text{res}_{t=\infty} F(t) = 0$ . By determining the residue of the function  $F(t)$  at infinity, we get

$$-a_1 + a_2 - 2a_3 + a_4 - a_5 = 0. \quad (37)$$

If the mapping parameters satisfy conditions (36), (37), then

$$f(t) = \int F(t) dt = \alpha \ln(t - a_1) - \alpha \ln(t - a_5) - \frac{\beta}{t - a_3} + t.$$

The well-known geometric characteristics of the flow region make it possible to write down three more equalities

$$l_1 = \text{Re}[f(1) - f(-1)] \cdot A; \quad l_2 = \text{Re}[f(a_4) - f(a_2)] \cdot A; \quad l_3 = \text{Re}[f(a_2) - f(-1)] \cdot A.$$

Given that  $A = h/\alpha\pi$ , and introducing new notations  $l_1/h = \bar{l}_1, l_2/h = \bar{l}_2, l_3/h = \bar{l}_3$  we get three equations that are missing to determine the five mapping parameters  $a_j, j=1,2,\dots,5$

$$\text{Re}[f(1) - f(-1)] - \bar{l}_1 \alpha \pi = 0; \quad (38)$$

$$\text{Re}[f(a_4) - f(a_2)] - \bar{l}_2 \alpha \pi = 0; \quad (39)$$

$$\text{Re}[f(a_2) - f(-1)] - \bar{l}_3 \alpha \pi = 0. \quad (40)$$

Now it is necessary to solve a system of five nonlinear equations (35), (36), (38)-(40) with respect to five mapping parameters. The main difficulty in solving this system by the Newton method is the ordering of parameters:

$$-1 < a_1 < a_2 < a_3 < a_4 < a_5 < 1$$

The point is that the method iterations regularly violate this ordering. To preserve it, we use the technique proposed in [18] (see also [19]). We introduce new variables

$$b_i = \ln \frac{a_i - a_{i-1}}{a_{i+1} - a_i}, \quad i = \overline{1,5}, \quad a_0 = -1, \quad a_6 = 1. \quad (41)$$

We turn the last equalities to variables  $a_i$ , for this we solve the following system of linear equations with a tridiagonal matrix

$$a_i - a_{i-1} - e^{b_i} (a_{i+1} - a_i) = 0, \quad \text{where } i = \overline{1,5}.$$

Solving this system of equations in the *Mathematica* package, we obtain

$$a_i = G_i(b_1, b_2, \dots, b_5), \quad i = \overline{1, 5}. \quad (42)$$

where functions  $G_i$  are built explicitly.

Now, taking into account equalities (42), we transform the system of equations (35), (36), (38)–(40), solving which we find the mapping parameters. Note that variables  $b_i$  are unordered, but any set of them gives an ordered set of variables  $a_i$ . When applying the Newton method to the transformed system, the zero values of variables  $b_i$  were simply chosen as the zeroth approximation, and the iteration process was always converged.

Thus, we have an opportunity to construct a function

$$f(t) = \int F(t)dt = \alpha \ln(t - a_1) - \alpha \ln(t - a_5) - \frac{\beta}{t - a_3} + t$$

and conformal mapping

$$z(t) = A[f(t) - f(-1)] \quad (43)$$

Now we calculate the adjoined flow rate through the slotted openings in the walls of duct. In the parametric plane, we have sources at points  $A_1$  ( $t = a_1$ ),  $A_3$  ( $t = a_3$ ),  $A_7$  ( $t = \infty$ ) and stock at point  $A_5$  ( $t = a_5$ ). The complex potential  $w = \phi + i\psi$  of such a flow will be equal to

$$w = \frac{q}{\pi} \ln(t - a_1) - \frac{(q + q_1 + q_2)}{\pi} \ln(t - a_5) + \frac{q_2}{\pi} \ln(t - a_3), \quad (44)$$

where  $\phi$ ,  $\psi$  are potential and function of flow,  $q_1$  and  $q_2$  are flow rates through the corresponding slotted openings,  $q = v_\infty h$  is the transit flow rate. We find the derivative

$$\frac{dw}{dt} = \frac{q}{\pi(t - a_1)} - \frac{q_1 + q_2 + q}{\pi(t - a_5)} + \frac{q_2}{\pi(t - a_3)}.$$

At points  $A_0$ ,  $A_2$  velocities are limited and therefore  $dw/dt$ ,  $dw/dt = 0$ . We solve the system of equations

$$\begin{cases} \frac{dw}{dt}(t = -1) = \frac{q}{\pi(-1 - a_1)} - \frac{q_1 + q_2 + q}{\pi(-1 - a_5)} + \frac{q_2}{\pi(-1 - a_3)} = 0; \\ \frac{dw}{dt}(t = a_2) = \frac{q}{\pi(a_2 - a_1)} - \frac{q_1 + q_2 + q}{\pi(a_2 - a_5)} + \frac{q_2}{\pi(a_2 - a_3)} = 0 \end{cases}$$

with respect to  $q_1$  and  $q_2$ . As a result, we obtain

$$q_1 = \frac{q(a_3 - a_1)(a_5 - a_1)}{(1 + a_1)(a_2 - a_1)}, \quad q_2 = \frac{q(a_3 + 1)(a_3 - a_2)(a_1 - a_5)}{(1 + a_1)(a_2 - a_1)(a_3 - a_5)}.$$

Now we can calculate the adjoined flow rate, which we present in the dimensionless form

$$C_q = \frac{q_1 + q_2}{q} = \frac{(a_3 - a_1)(a_5 - a_1)}{(1 + a_1)(a_2 - a_1)} + \frac{(a_3 + 1)(a_3 - a_2)(a_1 - a_5)}{(1 + a_1)(a_2 - a_1)(a_3 - a_5)}. \quad (45)$$

The problem for a viscous fluid was also solved numerically in the Flow3d software package. The boundary conditions were formulated in the same way as in Problem 1. The calculation results are presented below.

### 3. Results and Discussion

#### 3.1. Hole on one side of the intake duct wall

During the calculations, we also determined the dimensionless adjoined flow rate  $C_q$  and the jet contraction coefficient  $K$ . Figure 6 shows graphs of the corresponding dependences (19) and (22). Recall that the parameters  $b$  and  $c$  at given values  $l/h$  are determined by formulas (24), (28). The dashed line shows the graph  $C_q$  for the flow, where the flow separation at point  $A$  is not taken into account.

Comparison of graphs shows that separation of flow reduces the adjoined flow. We also see that the jet contraction coefficient tends to 0.5 with an increase in the length of the gap, that is, the flow in the channel becomes close to the flow in the Bord nozzle [17].

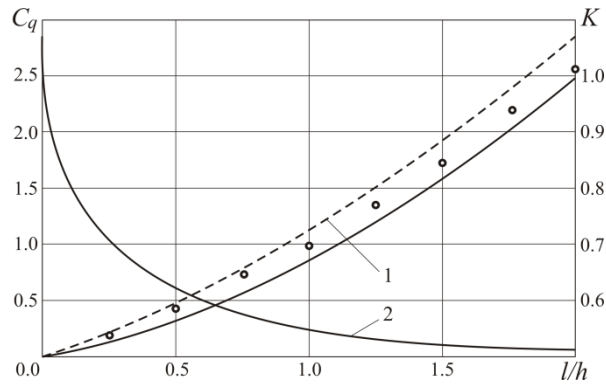


**Figure 6. Function graphs: 1 – adjoined flow taking into account flow separation (solid line), without taking into account flow separation (dashed line), 2 – jet contraction coefficient, ( $C_q$  values obtained numerically in the *Flow3d* program are shown by circles).**

Using the mapping formula (29), the streamlines' coordinates in the physical plane are determined. Similarly, the intake flow streamlines are constructed, but a semicircle of small radius  $C_b$  is constructed around point  $B$  ( $t = b$ ). Figure 5a shows the streamlines constructed in the described way for various values of  $l/h$ .

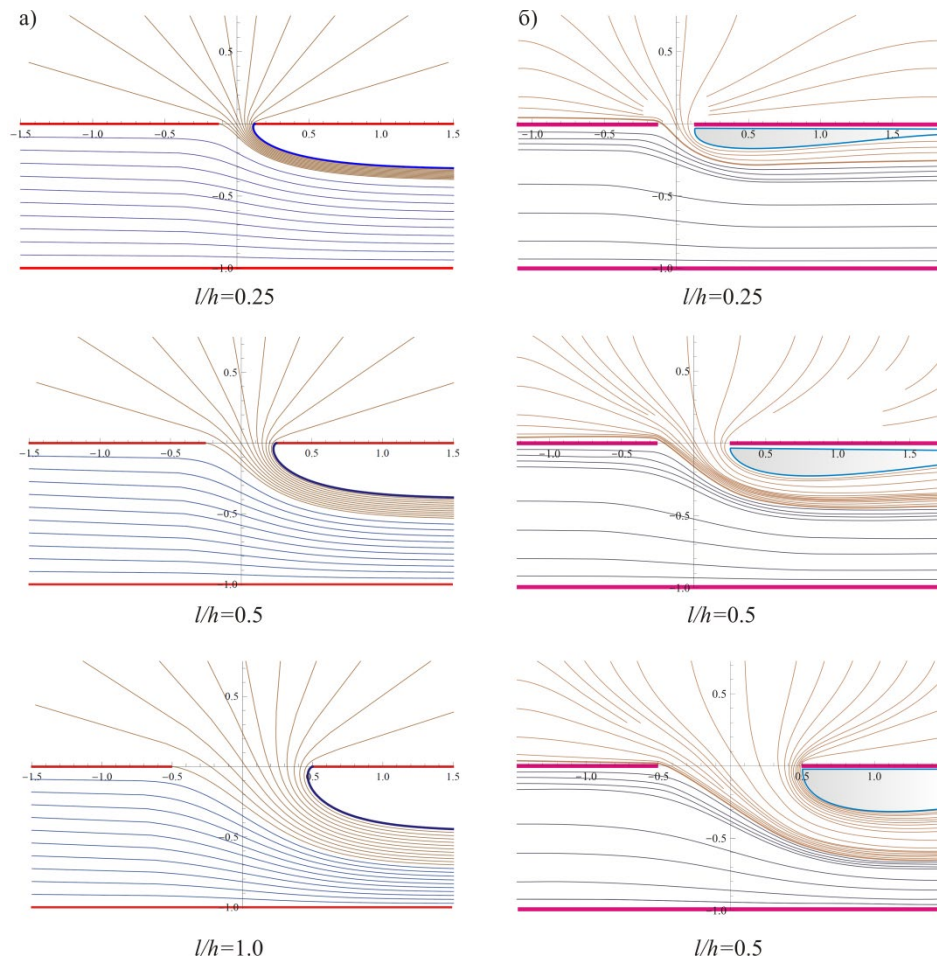


**Figure 7. Flow lines near the hole in one wall of the duct: a – analytical solution in NDSolve program of Mathematica software, b – numerical solution in the Flow3d program**

### 3.2. Double-sided intake panel element

Figure 8 presents a graph of dependence of  $C_q$  on the device geometry. Minimum of  $C_q$  is achieved for opposed openings. As the gap between the slots increases, the adjoined flow tends to a constant value.

The intake rate is minimal with the opposite arrangement of openings, with an increase in the spacing it increases. Starting from a distance  $\bar{l}_3 = 2$ , it reaches its maximum value and then remains constant. That is, it can be argued that at  $\bar{l}_3 > 2$  the mutual influence of the openings disappears.

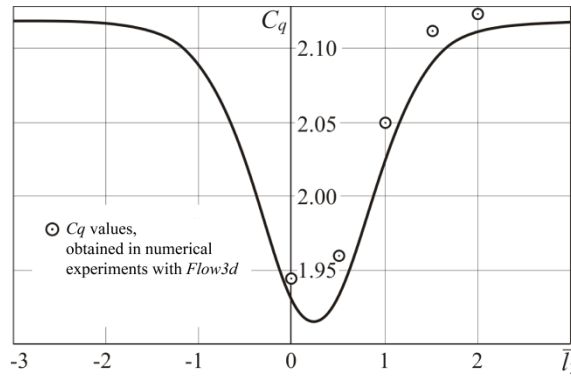


**Figure 8. The graph of dependence of the adjoined flow from the spacing between openings  $\bar{l}_1 = 1, \bar{l}_2 = 0.5$ .**

Knowing the complex potential (44) and the conformal mapping formula (43), we can further construct the flow streamlines in the physical domain. Figure 9a shows the flow map for different locations and sizes of slot openings.

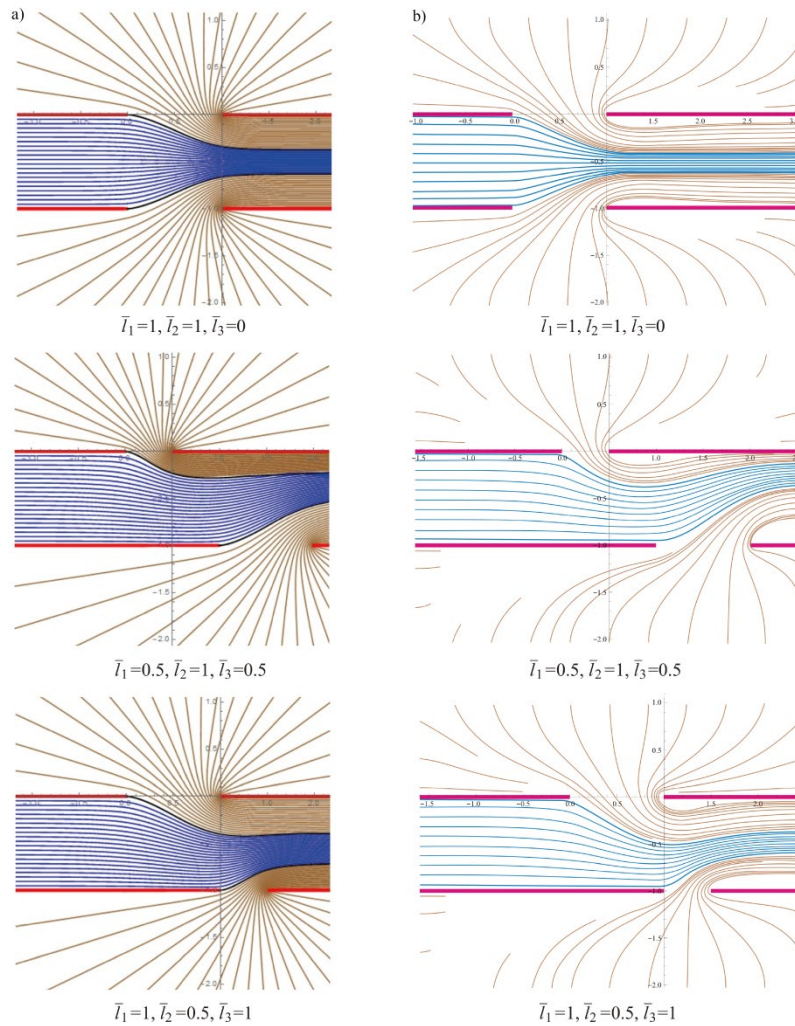


**Figure 9. Flow streamlines in openings on opposite walls of the duct: a – analytical solution in the NDSolve program of Mathematica package, b – numerical solution in the Flow3d program.**

The intake rate is minimal with the opposite arrangement of holes, with an increase in the spacing it increases. Starting from a distance  $\bar{l}_3 = 2$ , it reaches its maximum value and then remains constant. I.e. it



can be argued that with  $\bar{l}_3 > 2$  the mutual influence of the cracks disappears. Considering the complex potential (44) and the conformal mapping formula (43), we can further construct the flow streamlines in the physical domain. In Figure 9a a flow pattern for different locations and sizes of slit openings is shown. Pictures of flows constructed by Flow3d software package are shown in Figure 9, b.

The results of calculating the attached flow are shown by dots in Figure 8. We can state the accordance between analytical and numerical calculations

The numerical method allows to obtain more physics of the flow and, in particular, determines the geometry of the stagnant zone formed when the flow is cut off from sharp edges. Within the framework of the used analytical model, the shape of the stagnant zone is not determined.

The problem was also solved numerically in the *Flow3d* software package. The boundary conditions were formulated in the same way as in Problem 1. The flow maps constructed using the *Flow3d* software package are shown in Figure 9, b. The results of calculating the adjoined flow are shown by dots in Figure 8. We can state a good agreement between analytical and numerical calculations.

The numerical method allows one to obtain a more physical picture of the flow and, in particular, it determines the geometry of the stagnant zone formed when the flow is cut off from sharp edges. Within the framework of the used analytical model, the shape of the stagnant zone is not determined.

#### 4. Conclusions

In the work, the velocity field created by the action of the slotted hole on the duct wall, as well as at the intake panel with a two-sided arrangement of slotted holes, is analytically and numerically calculated. In the framework of the inseparable and detached models of potential ideal fluid flows, equations for the flow streamlines are obtained. The flow patterns are compared with the results of numerical calculations performed for a viscous fluid. The intensity of absorption is determined depending on the width of the slit and the flow rate.

Important results have been obtained that can be used in the design of air duct systems:

- the flow rates of air entering through the slots in the walls of the duct are determined, depending on their width, relative position and transit flow value;
- current flow lines are constructed;
- it was found that the intake intensity is minimal with the opposite arrangement of slots;
- The shape and size of the stagnant zones are determined numerically.

It should be noted that the qualitative patterns of the flows obtained by analytical and numerical methods are slightly different, since the flow model underlying the analytical calculation does not imply that the boundaries of the stagnant zone are closed on the duct wall. The values of the attached flow, determined analytically and numerically, practically coincide.

The results of the experimental determination of the flow characteristics and the intensity of absorption through the openings for the considered geometric situations are being prepared for publication. In particular, Figure 10 shows photographs of the boundaries of the separation zones at the middle suction inlet in a rectangular duct at  $l/h = 0.32$ . The experiments were run by Ph.D. Ziganshin A.M. in the laboratory of Kazan State University of Architecture and Engineerin (KSUAE).

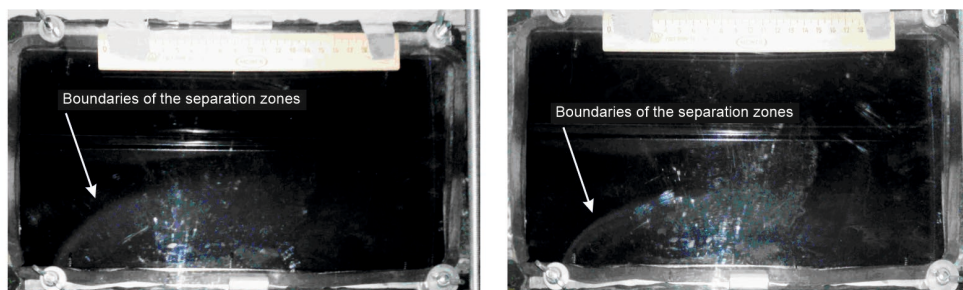


**Figure 10. Boundaries of the separation zones at the middle intake hole in a rectangular duct at  $l/h = 0.32$  at different velocity of the transit flow.**

#### References

1. Altuntas, O., Sogut, M.Z., Yalcin, E., Karakoc, T.H. Assessment of thermodynamic and environmental performances in subcooling process for different refrigerants. *International Journal of Exergy*. 2017. 24 (2-4). Pp. 216–234. DOI: 10.1504/IJEX.2017.087655.
2. Singh, L., Singh, S.N., Sinha, S.S. Effect of standoff distance and area ratio on the performance of circular exhaust ejector using computational fluid dynamics. *Proceedings of the Institution of Mechanical Engineers, Part G: Journal of Aerospace Engineering*. 2018. 232 (15). Pp. 2821–2832. DOI: 10.1177/0954410017717287.

3. Singh, L., Singh, S.N., Sinha, S.S. Effect of Slot-Guidance and Slot-Area on Air Entrainment in a Conical Ejector Diffuser for Infrared Suppression. *Journal of Applied Fluid Mechanics*. 2019. 12(4). Pp. 1303–1318. DOI: 10.29252/jafm.12.04.29593.
4. ASHRAE. 2017 ASHRAE handbook : fundamentals. ASHRAE handbook : fundamentals2017.
5. Goodfellow, H.D., Tähti, E. PREFACE. *Industrial Ventilation Design Guidebook2001*. San Diego, CA: Academic Press. 1555 p.
6. Logachev, I.N., Logachev, K.I., Averkova, O.A., Azarov, V.N., Uvarov, V.A. Methods of Reducing the Power Requirements of Ventilation Systems. Part 4. Theoretical Prerequisites for the Creation of Dust Localizing Devices with Swirling Air Flows1. *Refractories and Industrial Ceramics*. 2014. 55(4). Pp. 365–370. DOI: 10.1007/s11148-014-9728-6.
7. American Conference of Governmental Industrial Hygienists. *Industrial ventilation : a manual of recommended practice for operation and maintenance2007*.
8. Burgess, W.A., Ellenbecker, M.J., Treitman, R.D. *Ventilation for Control of the Work Environment: Second Edition*. 2004. Wiley-Interscience. 443 pp.
9. Cao, Z., Wang, Y., Duan, M., Zhu, H. Study of the vortex principle for improving the efficiency of an exhaust ventilation system. *Energy and Buildings*. 2017. 142. Pp. 39–48. DOI: 10.1016/j.enbuild.2017.03.007.
10. Yang, Y., Wang, Y., Song, B., Fan, J., Cao, Y. Stability and accuracy of numerical investigation of droplet motion under local ventilation airflow. *Building and Environment*. 2018. 1470. Pp. 32–42. DOI: 10.1016/j.buildenv.2018.05.023.
11. Koshkarev, S., Azarov, V., Azarov, D. The Decreasing Dust Emissions of Aspiration Schemes Applying a Fluidized Granular Particulate Material bed Separator at the Building Construction Factories. *Procedia Engineering*. 2016. 165. Pp. 1070–1079.
12. *Handbook of Hydraulic Resistance*, 3rd Edn. By I.E. Idelchik. Begell House, *Journal of Fluid Mechanics*. 1994. 790 pp.
13. ANSYS. ANSYS FLUENT User's Guide 2013.
14. FLOW-3D® User's Manual, Version 9.3, Flow Science, Inc., (2008).
15. Cordes, G.M.I. Gurevich, The Theory of Jets in an Ideal Fluid. (International Series of Monographs in Pure and Applied Mathematics, Volume 93) VIII + 412 S. m. 262 Abb. Oxford/London/Edinburgh/New York/Toronto/Paris/Braunschweig 1966. Preis geb. £ 5 net. Pergamon . ZAMM – Zeitschrift für Angewandte Mathematik und Mechanik. 1967. DOI:10.1002/zamm.19670470418.
16. Santalo, L.A. Book Reviews: – 1. Conformal Mapping: Methods and Applications: R. Schinzinger and P.A.A. Laura Elsevier Amsterdam, Oxford, New York, Tokyo 1991. 581 p.
17. Logachev, I.N., Logachev, K.I., Averkova, O.A., Azarov, V.N., Uvarov, V.A. Methods of Reducing the Power Requirements of Ventilation Systems. Part 4. Theoretical Prerequisites for the Creation of Dust Localizing Devices with Swirling Air Flows1. *Refractories and Industrial Ceramics*. 2014. 55. Pp. 365–370. DOI: 10.1007/s11148-014-9728-6.
18. Elcrat, A.R., Trefethen, L.N. Classical free-streamline flow over a polygonal obstacle. *Journal of Computational and Applied Mathematics*. 1986. 14(1-2). Pp. 251–265. DOI: 10.1016/0377-0427(86)90142-1.
19. Maklakov, D.V., Valitov, R.R., Posokhin, V.N., Safiullin, R.G. Calculation of intensity of air absorption through the openings in the side wall of air line. message 2. *Journal «Izvestiya vuzov. Investitsiyi. Stroyitelstvo. Nedvizhimost»*. 2018. 8(1). Pp. 160–167. DOI: 10.21285/2227-2917-2018-1-160-167.
20. John D. Anderson *Fundamentals of Aerodynamics: Fifth edition*. 2011. 1106 p.

### **Contacts:**

*Dmitry Maklakov, dmaklak@kpfu.ru*

*Vladimir Posohin, posohin@mail.ru*

*Rinat Safiullin, safiullin\_rinat@mail.ru*

*Julia Kareeva, jkareeva2503@gmail.com*

© Maklakov, D.V., Posohin, V.N., Safiullin, R.G., Kareeva, J.R., 2020